J Solid State Electrochem (2012) 16:1193–1202
DOI 10.1007/s10008-011-1498-1

ORIGINAL PAPER

Electrochemical response of natural and induced passivation of high strength duplex stainless steels in alkaline media

Mercedes Sánchez · Hitham Mahmoud · Maria Cruz Alonso

Received: 28 January 2011 / Revised: 16 June 2011 / Accepted: 30 June 2011 / Published online: 29 July 2011

Abstract The passivation of two high strength duplex stainless steels (HSSS) was investigated in alkaline solutions simulating the pore solution of concrete by the growth of natural and induced passive films. Induced passive films were generated both by cyclic voltammetry and by chronoamperometry. Natural passive films were spontaneously grown by the immersion of the steel in the alkaline electrolyte. These passive layers were characterised by electrochemical impedance spectroscopy, corrosion current density (i_{corr}) and corrosion potential (E_{corr}) monitoring. The effect of significant parameters, such as the pH in the HSSS/alkaline solution interface, the composition of the duplex stainless steels and the ageing of the passive layer, on the electrochemical performance of both induced and spontaneously grown passive films has been analysed. The increase of alkalinity highly influences the electrochemical performance of the passive film by promoting the formation of a passive layer with a less resistant electrochemical response. The electrochemical behaviour of the passive layer is also affected by the alloying elements like Mo or Ni. Both natural and induced passive films show similar electrochemical trend with respect to significant parameters such as the pH and the composition of the steel. The ageing of the spontaneously grown passive layer promotes a higher resistive electrochemical response which might be related to the enrichment of the passive layer in non-conducting (or semi-conducting) oxides.

Keywords High strength duplex stainless steels · Alkaline media · Passivation · Mo-alloy · Electrochemical techniques

M. Sánchez (✉) · H. Mahmoud · M. C. Alonso
Research Centre of Safety and Durability of Structures and Materials (CISDEM) UPM-CSIC,
C/ Serrano Galvache 4,
28033 Madrid, Spain
e-mail: mercesanc@ietcc.csic.es

Introduction

The high corrosion resistance of stainless steels (SS) is attributed to the formation of protective oxide layers allowing their use in very different scenarios, from acid to alkaline environments and even in presence of high Cl^- contents. The properties and the composition of the passive layer control the corrosion response of the SS.

The passivation of SS is a complex process influenced by several parameters, such as the alloy composition, the environment, and the conditions of passive layer formation [1–6]. The electrochemical properties of passive SS have been widely studied from passive layers grown under controlled conditions (potentiostatic or potentiodynamic tests) [6–9]. A double-layered structure constituted by an inner p-type and an outer n-type layers with a mixed semiconductive behaviour has been proposed for the passive layers formed under these conditions [7–10]. The electrochemical behaviour of the passive film is influenced by the incorporation of alloying elements, like Ni and Mo [11, 12]. Alloying elements in the composition of the steel modify the electrochemical properties of the oxides forming the double-layered passive film [4–7, 13–16], even affecting the susceptibility of the SS to suffer from pitting corrosion. In fact, stainless steels with high Mo and Ni content have showed higher resistance against pitting corrosion [13, 17, 18].

Stainless steels are also employed as reinforcements (SSR) exposed to the alkaline nature of the concrete [19–21]. In this case, the study of the SS passivation process and the modelling of the passive layer growth become relevant for further considerations concerning the durability of reinforced concrete structures. Most of the studies focussed on addressing the passivation mechanism of RSS have been carried out inducing the formation of passive films in alkaline solutions under accelerated conditions [22–24]. The electrochemical

behaviour of induced passive layers should reproduce the response of spontaneously grown passive layers to make suitable this type of testing in concrete studies. However, the investigations carried out considering the natural formation of the passive films on SS surface in alkaline media are still scarce [3, 25–27], and the existing studies have been mainly performed in solutions but not in cementitious materials. Few of them have considered the effect of influencing factors, such as the pH and the type of stainless steel, on the composition and on the electrochemical response of the passive layer [3, 22]. A mixed double-layered magnetite (mixed Fe^{II}/Fe^{III} oxide)-hematite (Fe^{III} oxide) structure evolving to hematite with the natural ageing and the pH decrease have been reported for the Fe-oxide part of the passive layer both on SS [3, 24, 26] and on carbon steels [28].

High strength stainless steels (HSSS) are obtained after a cold drawing process from the parent SS. At least 50–70% of reduction is needed for a HSSS [29, 30]. The cold drawing process increases the tensile strength and the 2% proof stress of the SS and induces changes in the microstructure of the SS (e.g., deformation in the grain size). The austenite to martensite transformation, with the consequent corrosion resistance reduction, has been reported for some type of austenitic SS with low content of alloying elements [31].

However, no studies exist concerning the influence of these modifications on the electrochemical response of HSSS when exposed to an alkaline environment such as that of concrete. Indeed, the effect of Mo on the corrosion behaviour of duplex HSSS is a subject of interest for a better understanding of the passivation and of the pitting corrosion processes in this type of steels. In present paper, the interest is focused on studying the influence of significant parameters such as the pH and the presence of alloying elements, especially Mo content, in the passivation of cold-drawn duplex-SS (HSSS). The research analyses the electrochemical response of natural and induced passive films of duplex HSSS in alkaline solutions simulating the environmental conditions of the concrete pores. Although these are simplified systems that are just indicative of the actual behaviour of real concrete environments, they are more feasible for understanding the passivation mechanisms involved. The influence of the SS/alkaline solution of concrete pores interface on the passivation process has been simulated by considering different alkaline electrolytes.

Experimental procedure

Specimens: chemical composition and surface preparation

Two high strength duplex stainless steels, 1.4462 and 1.4362, wires of 4 mm in diameter were studied. The chemical composition and the mechanical properties of both stainless steels are given in Tables 1 and 2 respectively.

The microstructural changes induced by the cold drawing process have been identified by comparing the polished surfaces of the parent and the cold-drawn stainless steels after a chemical etching in 30 ml HCl (36%)+10 ml HNO_3 (70%)+10 ml methanol (96%) for 30 s. Very fine austenitic grains can be identified in the initial duplex SS (parent), as observed in Fig. 1a for both SS (up for 14362 and down for 14462), while a more refined microstructure is observed in the case of the cold-drawn SS, as seen in Fig. 1b (up for 14362 and down for 14462).

Testing conditions

Two solutions were considered to simulate the different alkalinity at the SS/concrete interface:

1. Saturated $Ca(OH)_2$, pH 12.5
2. Saturated $Ca(OH)_2$+0.5 M KOH, pH 13.5

All tests were carried out at constant and controlled temperature (25 °C) under aerated conditions and without stirring.

Electrochemical measurements

The electrochemical experiments were performed in a three-electrode cell arrangement. A polyethylene cell stable in the high alkaline pH of the electrolyte was employed. Samples of 6 cm length were used as working electrodes and tested as received without polishing. An exposed area of 1.28 cm^2 was delimited with isolating tape. A graphite rod of 5 mm in diameter and 6 cm in length was used as counter-electrode. A standard saturated calomel electrode (SCE) was employed as reference electrode.

The ultrasound cleaning of the surface in water was carried out immediately before each electrochemical test. Different electrochemical techniques were employed to evaluate the steel response during the passive film formation. The electrical equipments to monitor the electrochemical interface of working elec-

Table 1 Chemical composition of 14462 and 14362 high strength duplex stainless steels in wt,%

	%C	%Cr	%Ni	%Mo	%Mn	%Si	% Fe
1.4462	0.04	23.3	4.3	3.7	2.1	0.60	Bal.
1.4362	0.03	22.9	4.29	0.1	1.79	0.60	Bal.

Table 2 Mechanical properties of 14462 and 14362 high strength duplex stainless steels

	1.4462		1.4362	
	Parent	Cold-drawn	Parent	Cold-drawn
Maximum stress, MPa	976	1,712	865	1,629
Yield strength, MPa	633	1,527	569	1,586
Young modulus (*E*), GPa	186	208	178	171

trode/alkaline solution were an ACM Gill AC potentiostat for the DC-measurements and an AUTOLAB PGSTAT30 potentiostat for the AC-measurements. Each electrochemical test was carried out on two samples to assure its reproducibility.

1. Cyclic voltammetry (CV): was applied to acquire qualitative information about the redox processes occurring on the induced passive layer grown under the applied potential sweep. A scan rate of 1 mV/s was used. The potential region from hydrogen evolution (−1.4 V_{SCE}) to oxygen evolution (+0.55 V_{SCE}) was taken into account. CV experiments were started at the cathodic limit. Each sample was cycled six times to evaluate the stability of the oxides compounding the passive layer by evaluating the relaxation of the redox process taking place in the generated passive layer.
2. Chronoamperometry: a constant potential in the passive potential range (−0.3 V_{SCE}) was applied to evaluate the effect of pH and Mo content on the transient current, directly related with the structure of the induced passive films.
3. Corrosion potential (E_{corr}) and corrosion current density (i_{corr}) evolution: E_{corr} and i_{corr} of HSSS bars in the different alkaline media were periodically monitored during 20 days of immersion to analyse the ageing of the spontaneously grown passive film. The corrosion current density was calculated using the Stern–Geary equation [32] depending on the polarisation resistance (R_P) and the *B*-constant. The value of *B* was determined from the anodic and the cathodic Tafel slopes (b_a and b_c) in the potentiodynamic measurements performed after 2 h of immersion. A scan rate of 1 mV/s in the potential range from −0.2 to +0.2 V vs E_{OCP} [33] has been used.
4. Electrochemical impedance spectroscopy (EIS) measurements: were also carried out on the naturally grown passive layers at different ages of exposure, until 13 days of immersion. The measurements were recorded from 10 kHz to 1 mHz applying a signal of amplitude 10 mV_{rms} with potentiostatic control at the corrosion potential.

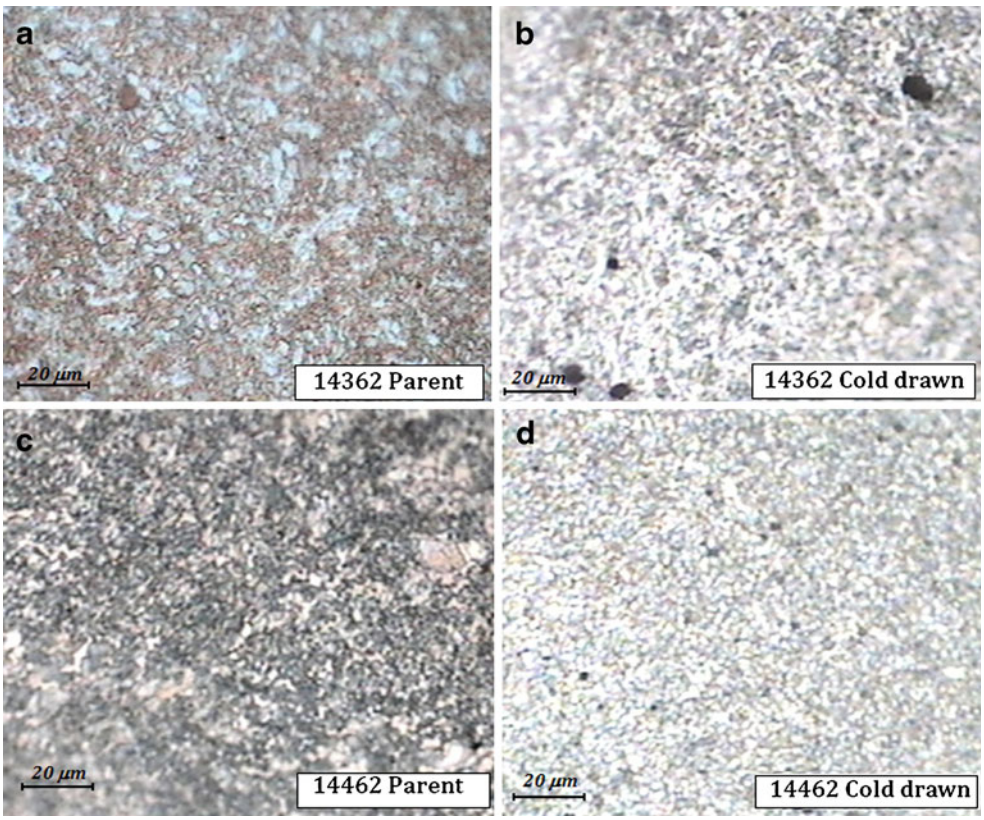

Fig. 1 Microstructure of both 14362 and 14462. **a** Parent steels, **b** Cold-drawn steels

Results

Electrochemical characterization of induced passive films

Cyclic voltammetry

The voltammograms with six cycles for 14462 and 14362 HSSS exposed to the pH 13.5 solutions have been represented in Figs. 2 and 3, respectively.

Three domains can be distinguished in both cases, and the features of the voltammograms can be summarised as follows:

(a) The potential domain from −1.4 to −0.55 V_{SCE}:

In this region a *peak I*, E=−1.1V_{SCE}, is observed in the anodic scanning. This peak, according to literature [22, 23], can be attributed to the redox process of Fe(II)-oxide formation. At more anodic potentials, a *peak II*, E=−0.75 V_{SCE}, can be identified. In literature, this peak is associated with the formation of magnetite (Fe_3O_4) from the Fe(II) oxidation [22, 23]. An increase of the current involved in *peak II* when increasing the number of cycles is observed (Figs. 2 and 3), indicating a possible accumulation of magnetite in the potentiodynamically induced passive film.

In addition to the iron redox processes occurring in this potential range, the redox processes of alloying elements also take place. The presence of the *peak I* (E=−1.1 V_{SCE}) is clearly observed in the first forward scan of HSSS 1.4462 (Fig. 2) but cannot be well identified for HSSS 1.4362 (Fig. 3) when it is immersed in the same alkaline solution. Furthermore, this peak tends to disappear with the number of potentiodynamic cycles. Analysing the differences found in both steels the interference of Mo redox process (Mo^0/Mo^{III}) on *peak I* can be expected. In fact, in agreement with Pourbaix [34], Mo^0/Mo^{III} may occur at similar potentials than iron oxidation Fe^0/Fe^{II} (E=−1.1 V_{SCE}).

(b) The potential domain from −0.55 to 0 V_{SCE}:

The low residual current densities measured in this potential range indicate that duplex HSSS have reached the passivity domain, and both stainless steels are able to generate a stable passive film in the tested alkaline solutions, as can be deduced from Table 3 where the mean values of the residual current registered in the passivity plateau have been summarised.

(c) The potential domain from 0 to +0.55V_{SCE}:

An increase on the current density is observed in this potential region, known as the transpassive domain. The main changes detected in this potential region for both HSSS are identified as follows:

The *peak III* has been assigned to the chromium oxidation process (Cr^{III}/Cr^{VI}) [23]. The current density decrease of the number of cycles (see Figs. 2 and 3) suggests the progressive formation of isolating Cr-oxides (III), mainly as Cr_2O_3, which decrease the reactivity of the passive layer. The *peak IV* appearing in the potential range +0.4 to +0.5 V_{SCE}, clearly observed in Fig. 2, has been associated to the redox process of Mo^{III} /Mo^{VI} according to Abreu et al.[22]. In present study, the *peak IV* is expected to correspond mainly to Mo^{III} /Mo^{VI} redox process as it is clearly observed only in the case of 14462 HSSS. The increase of the corresponding reduction *peak V*, identified at E=+0.29V_{SCE}, with the number of cycles would be a consequence of the passive layer enrichment in stable Mo-oxides. However, the contribution of Ni^{II}/Ni^{III} redox processes should not be neglected

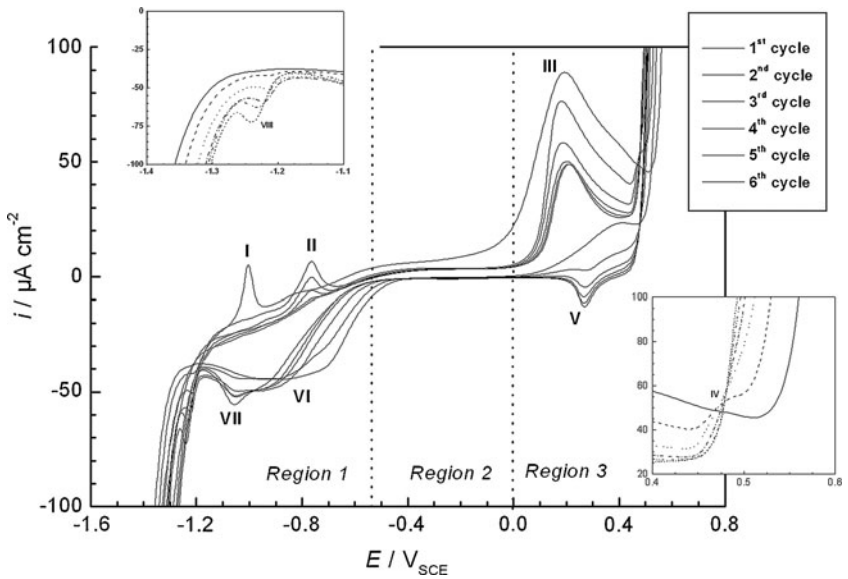

Fig. 2 Cyclic voltammograms of 14462 HSSS in solutions of saturated $Ca(OH)_2$+0.5 M KOH of pH 13.5 at 25 °C

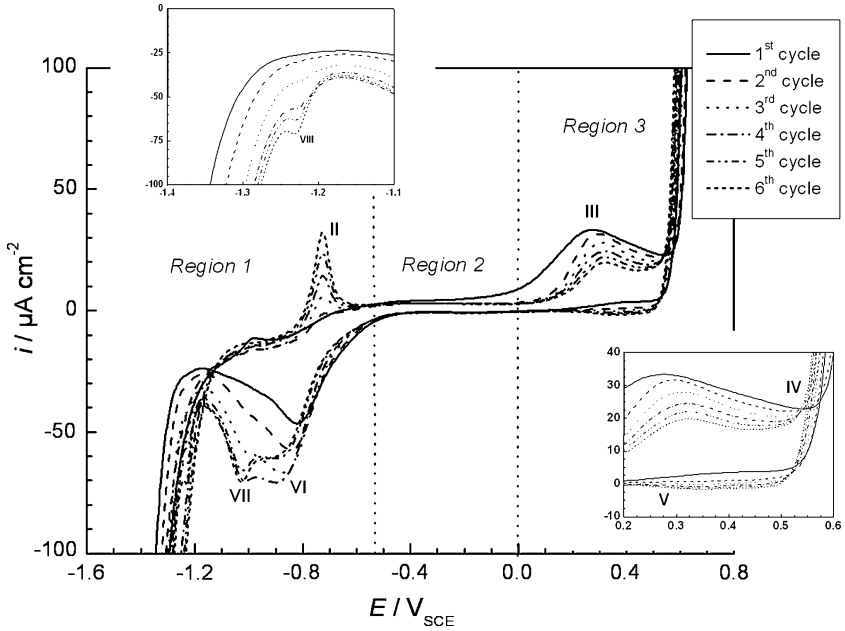

Fig. 3 Cyclic voltammograms of 14362 HSSS in solutions of saturated $Ca(OH)_2$+0.5 M KOH of pH 13.5 at 25 °C

as has been reported [22, 35] that both the anodic and the cathodic reactions take place at similar potentials than *peak IV* and *peak V*, respectively. In fact, a weak presence of peak V can also be identified in the case of SS 14362 without Mo (Fig. 3).

A sharp current anodic increase due to the oxygen evolution is registered at +0.5 V_{SCE}. A catalytic effect on the oxygen evolution process exerted by the nickel present in the external part of the passive film has been suggested by several authors [22, 23, 25]. This catalytic effect would explain the shift of oxygen evolution process to less anodic potentials after the first cycle. This shift on the oxygen evolution potentials (from +0.55 to +0.47 V_{SCE}) may hide the Ni^{II}/Ni^{III} oxidation peak, expected to occur at more anodic potentials

Chronoamperometry

The response of the passive layer potentiostatically induced at −0.3 V_{SCE} for the different pH has been analysed for the two duplex HSSS. The decay of current density with time during passivation at −0.3 V_{SCE} has been included in Fig. 4. The expression $i = A \cdot t^{-n}$ is proposed for the kinetic of passivation of Fe–Cr alloys [6] where n is the repassivation rate parameter and can be considered to be an indirect measure of the oxide growth on the SS surface. In Fig. 4, the fitting of experimental data to this expression has been represented with dotted lines.

The values of n as well as the steady-state current density for both duplex HSSS exposed to different alkaline media have been resumed in Table 4.

Independently of the HSSS type, smaller values of n are obtained when the pH increases. However, the presence of Mo in the composition of the HSSS promotes a significant increase of n. Values of n=1 has been associated to the formation of stable oxide films on a bare metal surface [36]. Then, in agreement with potentiodynamic results, the

Table 3 The residual current of the passivity domain of both stainless steels determined form the cyclic voltammograms

	1.4462		1.4362	
Residual current (µA cm^{-2})	pH 12.5	pH 13.5	pH 12.5	pH 13.5
Cycle 1	4.2	5.5	7.2	7.5
Cycle 6	2.7	3.2	2.9	3.9

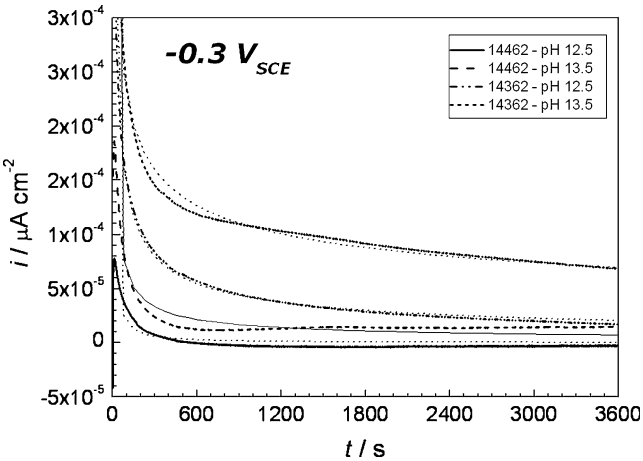

Fig. 4 Potentiostatic tests of 14462 and 14362 duplex HSSS at −0.3 V_{SCE}

Table 4 Significant parameters for the decay of current density during the passivation potentiostatically induced at −0.3 V_{SCE} of both HSSS considered

	n		i_{ss}, μA cm^{-2}	
	pH 12.5	pH 13.5	pH 12.5	pH 13.5
1.4462	1.090±0.010	0.617±0.003	4.3	7.9
1.4362	0.546±0.001	0.334±0.001	21.7	70.7

formation of a more stable passive layer is expected in presence of Mo while the increase of the alkalinity of the solution seems to promote the enrichment of the passive layer with more reactive oxides. The steady-state current density values give a similar response, with smaller values in presence of Mo and higher values of current density with the increase of pH.

Electrochemical characterization of natural passivation of HSSS

Corrosion potential and corrosion current density evolution

High strength stainless steels in concrete are spontaneously protected by forming a passive layer of stable oxides. Figure 5 shows the evolution of the corrosion potential with time for the two high strength duplex stainless steels exposed to alkaline electrolytes simulating the concrete pore solution.

The passive film growth takes place with the increase to more noble corrosion potentials observed during the earlier ages of immersion. Then, after 3 days of immersion, a stationary potential is reached due to the formation of a more stable passive film. E_{corr} values are affected by the pH as more anodic values are registered in smaller alkalinity.

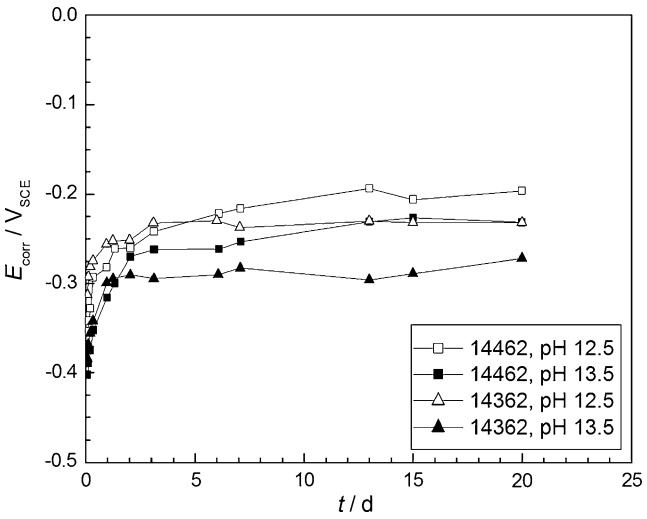

Fig. 5 Corrosion potential (E_{corr}) evolution of 1.4462 and 1.4362 during 20 days of immersion in solutions of pH 12.5 and 13.5 at 25 °C

Potentiodynamic polarisation curves were performed to calculate the B-constant value to be introduced in Stern–Geary equation. A Tafel-type behaviour has been considered to fit the curves:

$$i = i_0\left(10^{\frac{(E-E0,a)}{ba}} - 10^{\frac{(E-E0,c)}{bc}}\right) \quad (1)$$

Where b_a and b_c are the anodic and cathodic Tafel slopes, respectively, and the B-constant of Stern and Geary equation can be defined from these Tafel slopes:

$$B = \frac{b_a \cdot b_c}{2.303 \cdot (b_a + b_c)} \quad (2)$$

The fitting to Tafel behaviour by linear extrapolation of the cathodic and anodic branches starting at least at 0.05–0.1 V away from E_{corr} [35] gives the values of Tafel slopes. The electrochemical parameters estimated in the different situations (b_a, b_c and B-constant) are listed in Table 5. A mean value of 34 mV can be deduced for the B-constant and will be considered to determine i_{corr} from Stern-Geary equation.

The evolution of i_{corr} with the immersion time has been represented in Fig. 6, where a marked decay of i_{corr} with timing is registered during the first stages of exposure until a quasi-stationary value of i_{corr} is reached, after 4 or 6 days, depending on the pH (the stationary value is reached faster for lower pH).

Higher values of corrosion current density have been registered for both steels with the increase of the pH from 12.5 to 13.5. These higher values of corrosion current density may be related to a higher presence of more reactive oxides on the passive layer formed in the most alkaline solution [3, 26]. An agreement with the results obtained from induced passive layer can be deduced. For the same pH, the effect of Mo in stabilising the passive film can be inferred from the lower i_{corr} values measured for 14462 (higher content of Mo) comparing with 14362.

Electrochemical impedance spectroscopy evolution

The evolution of the Nyquist plots measured for 14462 HSSS at different immersion times in two different alkaline solutions (pH=13.5 and pH=12.5) is represented in Fig. 7a and b, respectively.

Table 5 The anodic and the cathodic Tafel lines slopes and the B constant value of 14462 and 14362 immersed in solution of pH 13.5 and 12.5

HSSS	pH	b_a, mV dec^{-1}	b_c, mV dec^{-1}	B, mV
14362	13.5	270	107	33
	12.5	287	96	31
14462	13.5	368	120	39
	12.5	270	102	32

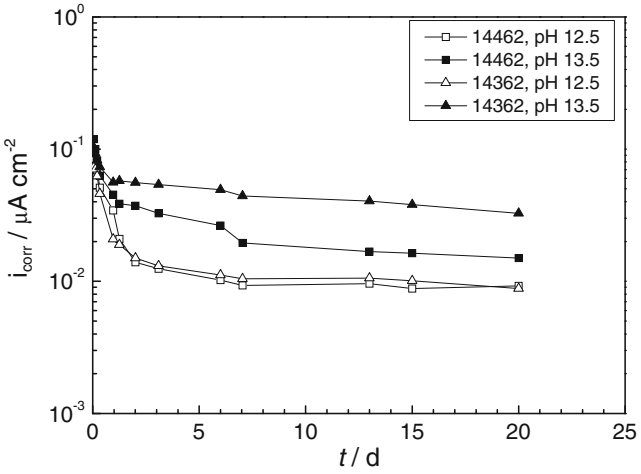

Fig. 6 Corrosion current density (i_{corr}) evolution of 1.4462 and 1.4362 stainless steels during 20 days of immersion in solutions of pH 13.5 and 12.5at 25 °C

The limit of impedance values at the low frequency range markedly increases during the first 3 days of immersion of the rebar in the alkaline media. However, an asymptotic tendency is observed after this period. It is accepted that this period of time is required to reach the steady-state conditions during spontaneous passivation of steel in alkaline media [3, 28] which is also supported by the E_{corr} and the i_{corr} measurements.

From the Bode diagrams of EIS results the presence of two time constants can be clearly identified. In Fig. 8, the Bode diagram of 14462 HSSS after 1 day of exposure to pH=12.5 has been included as an example.

The interpretation of EIS data in terms of equivalent electric circuits (EEC) is often considered in this type of studies. The EEC most commonly used [25, 27] for this system proposes two *R-CPE* (Constant Phase Element) loops in parallel, as schemed in Fig. 8.

The interpretation suggested for the elements of the circuit is the following: The time constant obtained at the higher frequencies is associated to the charge transfer resistance (R_{ct}) in parallel with the double-layer capacitance (C_{dl}). The low frequencies time constant (R_f·C_f) has been associated to the redox processes taking place in the oxide film. The fitting of experimental EIS data at the different times with simplex algorithm gives the evolution of the parameters involved in the EEC. The quality of the fitting for 14462 HSSS EIS results with the 2*RC* electrical equivalent circuit can be observed by comparing the experimental data (dots) and the fitted data (lines) included in Figs. 7 and 8.

In Fig. 9, the evolution of R_{ct} (Fig. 9a) and C_{dl} (Fig. 9b) with the immersion time has been represented.

R_{ct} increases with ageing in alkaline solutions (pH 12.5 and 13.5) for both HSSS, 14462 and 14362, revealing that the charge transfer processes become more difficult due to the growing of the passive film. The capacitance (C_{dl}) values, Fig. 9b, ranged between 52–49 µF cm^{-2}, are typical of double-layer capacitance. No significant effect due to the presence of Mo can be identified on the parameters of the highest frequencies time constant, R_{ct} or C_{dl}.

The time constant (R_f C_f) at lower frequencies suffers an important increase with ageing in alkaline solutions, as can be observed in Fig. 10. The influence of pH on this time constant can be also deduced from Fig. 10 as this time constant increases for lower pH values (pH 12.5).

Concerning the effect of Mo on this parameter, only at the lowest pH and after some days of immersion is possible to deduce slight differences between both types of HSSS. In this situation, according to i_{corr} evolution (Fig. 7), the passive layer is expected to be formed and stabilised.

Discussion

Formation of induced passive films on high strength duplex stainless steels

The redox processes occurring in the passive film induced in alkaline media are controlled both by the chemical

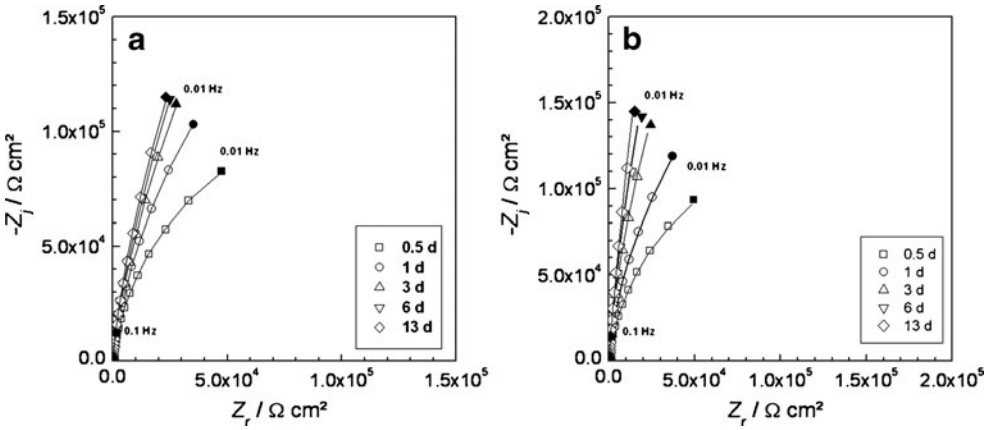

Fig. 7 Evolution of the impedance spectrum in Nyquist plots with immersion time (13 days) of 1.4462 in: **a** pH 13.5, **b** pH 12.5. Experimental data (*dots*), fitting with 2*RC* equivalent circuit (*solid lines*)

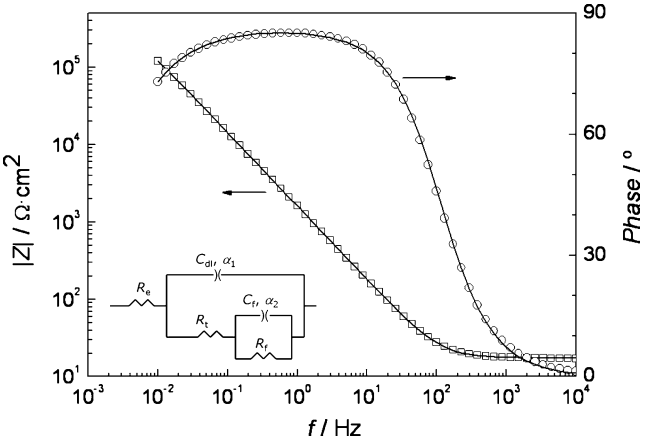

Fig. 8 Bode diagram for 14462 HSSS after 1 day of exposure to pH 12.5. Experimental data (*dots*), fitting with 2*RC* equivalent circuit (*solid lines*). Also included is the scheme of the equivalent electric circuit (EEC) used to simulate the EIS data

composition of the HSSS and by the pH of the surrounding environment, as can be deduced from Fig. 11 where the sixth cycle of the cyclic voltammetries carried out for both HSSS studied at the two different pH are represented. The increase of the alkalinity promotes higher current density values in the transpassive region, associated to the Cr^{III}/Cr^{VI} oxidation processes for both 14462 and 14362. These higher current density values might be related to the formation of more reactive Cr-oxides in the passive layer.

For the passive film formed on stainless steel in alkaline media, spinel-type structure with octahedral sites preferentially occupied by Cr^{III} and Fe^{II} has been reported elsewhere [25, 37]. The oxidation of Cr^{III} to Cr^{VI} species at the SS passive film/alkaline media interface is more favoured with the increase of pH. The depletion on Cr^{III} atoms in the spinel structure of the passive film can be compensated by incorporating atoms of Ni in the empty octahedral sites of the spinel that could explain the increase of the current density registered for the passive film formed at higher pH (13.5). In solutions of pH 12.5, the enrichment of Ni species in the spinel is not favoured, and smaller limit values of current density are obtained during the chronoamperometries (Fig. 4 and Table 4).

The Mo role in the electrochemical response of the passive film seems to be also influenced by the pH of the solution. The higher alkalinity could promote the accumulation of Mo-oxides in the passive film explaining in this way the increase of the reduction *peak V* (Fig. 2) observed at pH=13.5 but not identified at lower pH (pH=12.5). This effect is clearly observed when a and b of Fig. 11 are compared.

The contribution of Mo on the electrochemical response of the induced passive layer can be also deduced when potentiostatic transients are considered (Fig. 4 and Table 4). The reduction of the current density limit as well as the increase of the repassivation rate parameter, *n*, confirm the formation of more stable passive layer on stainless steels when the Mo-content of the composition increases.

Spontaneous passivation of high strength duplex stainless steels

In real conditions, the spontaneous passivation of HSSS takes place due to the alkaline nature of the concrete pore solutions. The decrease of the interfacial alkaline pH induces the formation of more stable passive films as can be deduced from the lesser values of the corrosion current density (Fig. 6) and the lower values of the time constant at the smallest frequencies (R_fC_f; Fig. 10).

The current decay has been attributed to a decrease in the Fe^{II}/Fe^{III} ratio in the passive film of steel in alkaline environments in agreement with [3, 24]. Moreover, the increase of the Cr^{III} content in the outer layer of the passive film promoting the enrichment in stable chromium oxide like Cr_2O_3 has been also reported with the decrease of the pH [5]. In a more alkaline interface, the formation of more oxidised chromium oxides (Cr^{6+}) and of less oxidised iron oxides, as Fe_3O_4, can explain the higher values of the corrosion current density registered (Fig. 7) as well as the decrease detected by EIS on the polarisation resistance values (Fig. 15).

For naturally grown passive films, duplex stainless steels with high Mo content should have higher content in chromium oxide species as suggested in Addari et al. [26]. The lower corrosion current density measured for

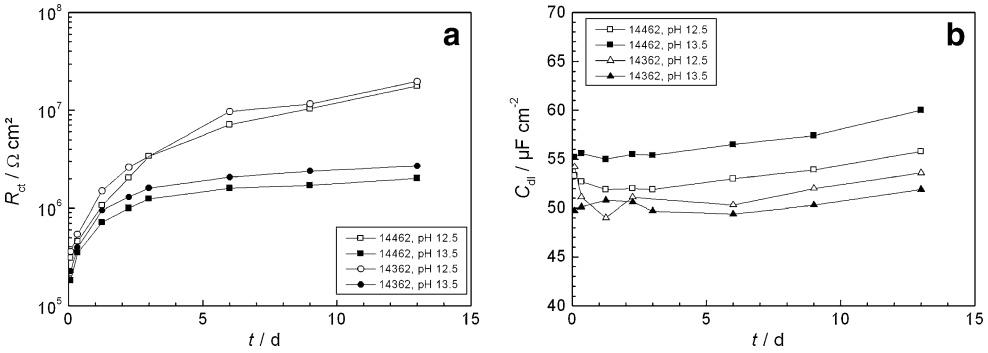

Fig. 9 Evolution with the immersion time of EEC parameters for 14462 and 14362 in solutions of pH 12.5 and 13.5. **a** Charge transfer resistance (R_{ct}), **b** Double-layer capacitance (C_{dl})

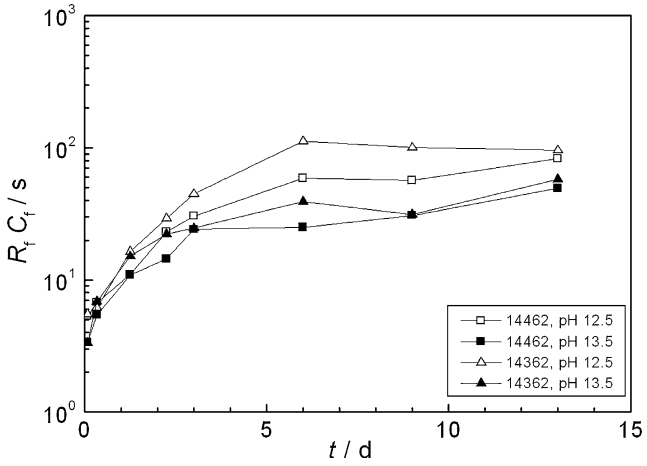

Fig. 10 Evolution of the time constant (R_f C_f) at the lowest frequencies of 14462 and 14362 with ageing in alkaline solutions of pH 12.5 and 13.5

14462 in present work suggests the formation of a more stable passive film when exposed to alkaline environments.

Ageing of passive layers of high strength duplex stainless steels exposed to alkaline solutions

The enhancement on the corrosion resistance of the duplex HSSS observed with their natural ageing in alkaline environments may be attributed to the changes in the thickness and the chemical composition of the film grown under these conditions [38] as confirms the increase of the charge transfer resistance (R_{ct}) with the exposure time (Fig. 9a).

The accelerated testing to induce the formation of a passive layer under potentiodynamic conditions (Figs. 2 and 3) shows that ageing in alkaline media by consecutive cycling promotes the transformation of Fe^{II} to Fe^{III} promoting a passive layer depleted in Fe^{II}. Also the stabilisation of the Cr-oxides with the number of cycles can be observed. Then, the formation of a more stable passive layer is expected with the ageing in alkaline media.

Moreover, the ageing of the passive film spontaneously grown on the stainless steel surface exposed to alkaline media modifies its chemical composition. Some authors [26] consider that the Fe^{II} content in the passive film decreases with ageing. Also, the evolution with ageing to a more stable passive film incorporating low soluble Ni oxides has been suggested by the same authors [26]. The decrease of the corrosion current density with time (Fig. 6) and the shift of the corrosion potential to more anodic potentials (Fig. 5) support this hypothesis that would be also confirmed by the EIS data through the increase of the R_fC_f time constant with time (Fig. 10).

Both induced and natural passive film formations on HSSS seem to be formed by a mix of oxides in different ratios that allow the different electrochemical response when the pH changes or depending on the Mo content. The stabilisation of the passive layer to a more oxidised level is favoured both by the presence of Mo and by the ageing of the passive layer. The influence of the pH when passive layers on HSSS are grown in alkaline media is also significant: passive layers enriched in more reactive oxides are formed when the alkalinity of the media increases.

Conclusions

The electrochemical response of two duplex HSSS exposed to alkaline solutions has been analysed both under controlled and natural conditions. The results allow concluding that:

- Both the pH of the solution and the composition of the duplex HSSS are significant parameters that control the electrochemical behaviour of the passive layer.
- The higher alkalinity of the environment surrounding the HSSS interface promotes the enrichment of the passive film in more reactive oxides.
- The presence of Mo in the composition of the SS allows the formation of more stable passive films attributed to changes in Fe-oxides and Cr-oxides.
- Similar electrochemical response has been deduced both for the induced and the natural passive layer.

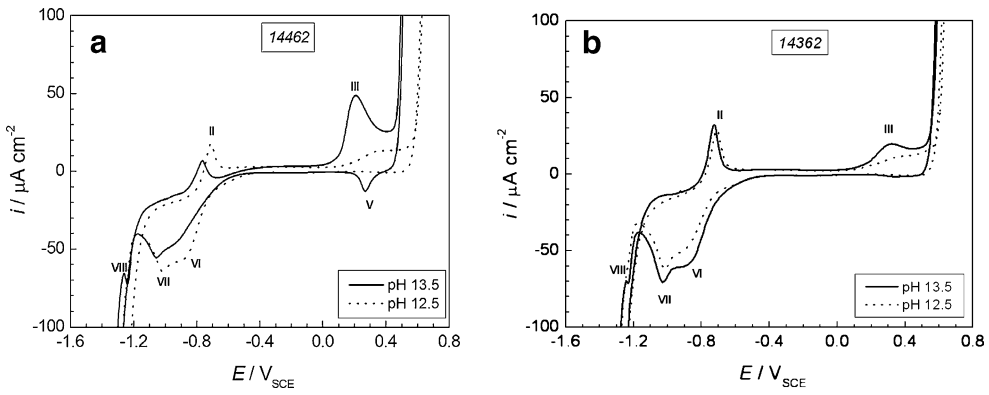

Fig. 11 Cyclic voltammograms (sixth cycle) of **a** 1.4462 and **b** 14362 stainless steels in solutions of pH 13.5 and 12.5

Acknowledgements Authors gratefully acknowledge the financial support from Spanish MICINN for the financial support given to this research in BIA2007-65394 project and also for the FPI given to H. Mahmoud. M. Sánchez acknowledges to Spanish Ministry of Education her post-doctoral position. The authors also acknowledge to INOXFIL for supplying of the HSSS.

References

1. Elsener B, DeFilippo D, Rossi A (1994) Modifications of passive films. In: Marcus P, Baroux B, Keddam M (eds.) EFC publ. No 12, The Institute of Materials, London, pp 6–11
2. Elsener B, Rossi A (1995) Mater Sci Forum 192–194:225–236
3. Freire L, Carmezim MJ, Ferreira MGS, Montemor MF (2010) Electrochim Acta 55:6174–6181
4. Bastidas JM, Torres CL, Cano E, Polo JL (2002) Corros Sci 44:625–633
5. Montemor MF, Simoes AM, Ferreira MGS, Da Cunha Belo M (1999) Corros Sci 41:17–34
6. Lee JB, Kim SW (2007) Mater Chem Phys 104:98–104
7. Kocijan A, Donik C, Jenko M (2007) Corros Sci 49:2083–2098
8. Lu YC, Clayton CR, Brooks R (1989) Corros Sci 29:863–880
9. Clayton CR, Lu YC (1986) J Electrochem Soc 133:2465–2473
10. Brooks AR, Clayton CR, Doss K, Lu YC (1986) J Electrochem Soc 133:2459–2464
11. Schmuki P, Böhni H (1992) J Electrochem Soc 139:1908–1913
12. Szklarska-Smialowska Z (2002) Corros Sci 44:1143–1149
13. Ameer MA, Fekry AM, El-Taib Heakal F (2004) Electrochim Acta 50:43–49
14. Boucherit N, Hugot-le Goff A, Joiret S (1992) Corrosion 48:569–579
15. Vignal V, Olive JM, Desjardins D (1999) Corros Sci 41:869–884
16. Tobler WJ, Virtanen S (2006) Corros Sci 48:1585–1607
17. Pardo A, Merino MC, Coy AE, Viejo F, Arrabal R, Matykina E (2008) Corros Sci 50:780–794
18. Ilevbare GO, Burstein GT (2001) Corros Sci 43:485–513
19. Castro-Borges P, de Rincón OT, Moreno EI, Torres-Acosta AA, Martínez-Madrid M, Knudsen A (2002) Mater Perform 41:50–55
20. Knudsen A, Jensen FM, Klinghoffer O, Skovsgaard T (1998) Cost-effective enhancement of durability of concrete structures by intelligent use of stainless steel reinforcement. In: Conference on Corrosion and rehabilitation of reinforced concrete structures, Florida, December 8–11
21. Klingghoffer O, Forlung T, Kofoad B, Knudsen A, Jensen FM, Skovsgaard T (2000) Practical and economical aspects of application of austenitic stainless steel , AISI 316, as reinforcement in concrete. In: Mietz J, Polder R, Elsener B (eds.) Corrosion of reinforcement in concrete, European Federation of corrosion, IOM Communications , London, pp 121–133
22. Abreu CM, Cristóbal MJ, Losada R, Nóvoa XR, Pena G, Pérez MC (2004) Electrochim Acta 49:3049–3056
23. Abreu CM, Cristóbal MJ, Losada R, Nóvoa XR, Pena G, Pérez MC (2006) Electrochim Acta 51:1881–1890
24. Abreu CM, Cristóbal MJ, Losada R, Nóvoa XR, Pena G, Pérez MC (2004) J Electroanal Chem 572:335–345
25. Bautista A, Blanco G, Velasco F, Gutiérrez A, Soriano L, Palomares FJ, Takenouti H (2009) Corros Sci 51:785–792
26. Addari D, Elsener B, Rossi A (2008) Electrochim Acta 53:8078–8086
27. Freire L, Carmezim MJ, Ferreira MGS, Montemor MF (2011) Electrochim Acta. doi:10.1016/j.electacta.2011.02.094
28. Sánchez M, Gregori J, Alonso C, García-Jareño JJ, Takenouti H, Vicente F (2007) Electrochim Acta 52:7634–7641
29. Nürnberger U, Wu Y (2008) Mater Corros 59:144–158
30. Wu Y, Nürnberger U (2009) Mater Corros 60:1–10
31. Rajan TV, Sharma CP, Sharma A (2006) Heat treatment-Principales and techniques Revised Edition, ISBE-81-203-0716-X. Prentice-Hall of Indian Private Limited, New Delhi, pp 48–51
32. Stern M, Geary AL (1957) J Electrochem Soc 104:56–63
33. Poorqasemi E, Abootalebi O, Peikari M, Haqdar F (2009) Corros Sci 51:1043–1054
34. Pourbaix M (1968) Atlas of Electrochemical Equilibrium in Aqueous Solution. Pergamon Press, Oxford
35. Kim JD, Pyun SI (1995) Electrochim Acta 40:1863–1869
36. Abreu CM, Cristóbal MJ, Losada R, Nóvoa XR, Pena G, Pérez MC (2008) Electrochim Acta 53:6000–6007
37. Abreu CM, Cristóbal MJ, Nóvoa XR, Pena G, Pérez MC, Rodriguez RJ (2002) Surf Coatings Tech 158–159:582–587
38. Kim JD, Pyun SI (1996) Corros Sci 38:1093–1102